Electronic Supplementary Material (ESI) for Nanoscale.
This journal is © The Royal Society of Chemistry 2017

—Supporting information available —

Key role of surface oxidation and reduction processes in the coarsening of Pt nanoparticles.

Eduardo Solano,[*a,b‡] Jolien Dendooven,[a‡] Ranjith K. Ramachandran,[a] Kevin Van de Kerckhove,[a] Thomas Dobbelaere,[a] Daniel Hermida-Merino[c] and Christophe Detavernier[a]

[a] *Department of Solid State Sciences, CoCooN, Ghent University, Krijgslaan 281/S1, 9000 Ghent, Belgium.*
[b] *Present address: NCD beamline, ALBA Synchrotron Light Source, Carrer de la Llum 2-26, 08290 Cerdanyola del Vallès, Spain.*
[c] *DUBBLE beamline, ESRF, Avenue des Martyrs 71, 38000 Grenoble, France*
[‡] *E.S. and J.D equally contributed to this work.*
[*] *Corresponding author: esolano@cells.es*

1 GISAXS analysis

The in situ acquired GISAXS patterns were analyzed following the methodology depicted in Fig. S.1. In brief, the data treatment consisted of analyzing the q_y position of the main scattering peak (Fig. S.1(a)) by taking a horizontal line profile through the GISAXS images (Fig. S.1(b)). This so-called horizontal q_y cut (taken at the qz position corresponding to the Yoneda region of the Si substrate) revealed the q_y position of maximum intensity ($q_{y,max}$). This treatment was repeated for each GISAXS image recorded at different temperatures during the annealing treatment (Fig. S.1(c)). The $q_{y,max}$ value was transformed from the reciprocal to real space by applying the $2\pi/q_{y,max}$ approximation, with D the average particle center-to-center distance (Fig. S.1(d)). Finally, from the known amount of Pt on the surface (obtained from XRF-RBS) and the distance D, the equivalent average spherical radius R was calculated for each GISAXS pattern.

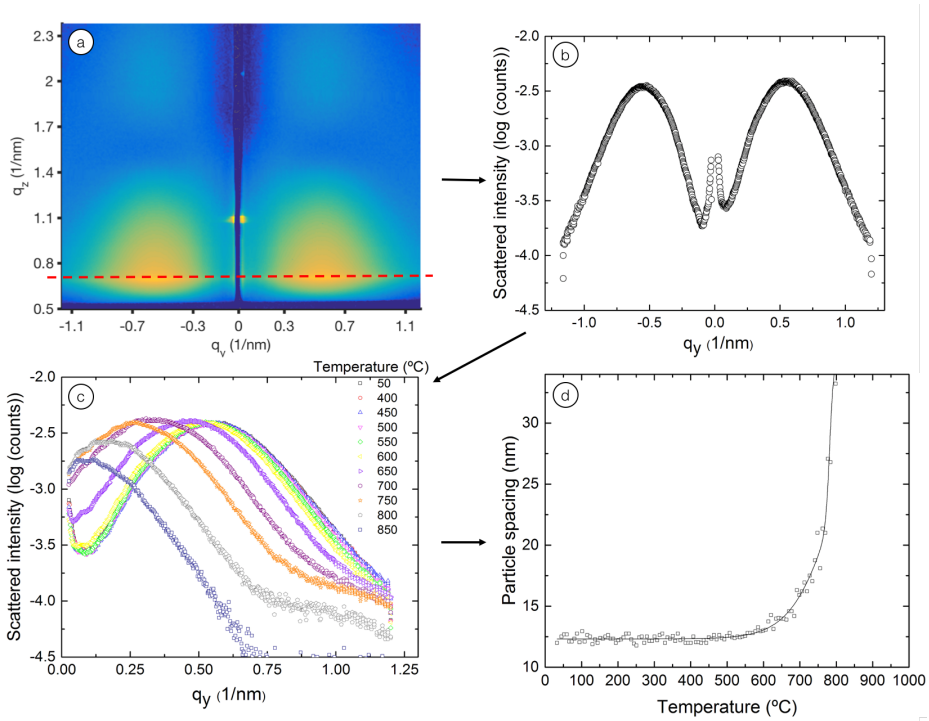

Figure S.1: Scheme summarizing the data treatment of the *in situ* GISAXS data. (a) Experimental GISAXS pattern. (b) Horizontal line profile extracted from the GISAXS patterns (red dashed line in (a)). (c) Combination of multiple line profiles realized on the patterns acquired at different temperatures. (d) The average center-to-center interparticle distance (D) as calculated by applying the $2\pi/q_{y,max}$ approximation.

The analysis of the patterns was semi-automated using a customized computing program. The workflow was as follows: first, the Yoneda peak position ($q_{z,max}$) was determined by finding the maximum of the scattering intensity in a user defined window in q-space (e.g. $0.05<q_y<1.5$ and $0.5<q_z<0.8$). Then, an horizontal line profile was taken at the $q_{z,max}$ position, integrating the signal over a q_z-range of 10 pixels. Because of the vertical symmetry of the pattern around q_y=0, only the positive q_y values were considered for analysis. Next, the maximum of the horizontal cut q_y cut ($q_{y,max}$) was determined. This value was then converted to the average center-to-center distance (D) between the nanoparticles by applying the $2\pi/q_{y,max}$ approximation. This process was repeated for the complete set of recorded GISAXS images, obtaining the evolution curve of the D spacing in function of the annealing temperature. Finally, the evolution in particle radius R during the thermal treatment was calculated by assuming a spherical particle shape and using the relation:

$D(nm) = \sqrt{\frac{\frac{4}{3}\pi r^3 \cdot 66.24(at./nm^3)}{S_{Pt}(at./nm^2)}}$

with the center-to-center particle distance (D), the Pt surface density S_{Pt} (calculated via XRF) and the bulk Pt density (66.24 nm^3).

2 GISAXS simulations for validation

To validate the above described fast analysis methodology, we employed simulations using the IsGISAXS software[1]. The GISAXS patterns of the as-deposited Pt-D sample and of the same sample annealed up to different temperatures (at 400, 600, 700 and 800 °C) were simulated. Vertical q_z and horizontal q_y line profiles at the $q_{y,max}$ and $q_{z,max}$ scattering lobe position were simulated and compared with the real line profile cuts. The simulations used the Distorted Wave Born Approximation (DWBA) with a Local Monodisperse Approximation (LMA) configuration. A graded interface was required to correct for the perturbation originating from the dense collection of particles on the surface[2]. The best agreement between simulations and experiment were obtained when assuming a two particle model consisting of 50 % full spheroids and 50 % hemi-spheroids for the Pt nanoparticles. The interference function was calculated based on the 1D paracrystal model, which is a regular 1D lattice with a loss of long-range order. The values for D and R obtained from the fast analysis were used as initial estimates of the nanoparticle spacing (D) and dimensions, with the particle radius (R) equal to R and the particle height (H) equal to 2R. A Gaussian function, described by the disorder parameter ω, was assumed for the distance (D) distribution. The particle radius (R) and height (H) distributions were chosen to be coupled, in the sense that a distribution of particle radii at constant height/radius ratio implies also a distribution of particle heights. A lognormal distribution was assumed for the particle radius (R), described by the dimensionless geometric standard deviation σR. The values for D, ω, R, H and σR were optimized to find the best agreement between the simulated GISAXS line profiles and the experimental ones. Then, the optimized values were used to simulate a full 2D GISAXS patterns.

Table S.1 lists the input parameters for the IsGISAXS calculations. Figure S.2 presents a comparison of the acquired and simulated patterns and the q_y and q_z cuts, demonstrating the good agreement between experiment and theory. Figure S.2 also shows complementary Fourier Fast Transform (FFT) analysis of representative SEM images, providing additional information on the average interparticle distance D. Table S.3 compares the results from the simulations with the values found via the fast analysis and FFT calculations of the corresponding SEM images. Table S.3 and Figure S.3 show the particle radius distributions for the selected GISAXS patterns. The adequate agreement between the different methodologies employed (Table S.3) validates the developed fast analysis strategy. Therefore, reliable values of the average interparticle center-to-center distance D and radius R can be directly extracted from the in situ data using the developed fast analysis method explained above.

Framework and beam parameters:

Framework: DWBA		Diffuse: LMA		Multilayer: 1		Number of index slices: 25		Polarization: ss
Beam Wavelenght:	Lambda (nm): 0.10332	$Wl_{dist.}$: none	Sigma Wl/Wl: -	Wl_{min}(nm): -	Wl_{max} (nm): -	nWl: 20	xWl: 3	
Beam $Alpha_i$:	$Alpha_i$(deg): 0.5	$A_{i,dist.}$: none	Sigma$A_{i,dist.}$ (deg): -	$A_{i,min}$ (deg): -	$A_{i,max}$ (deg): -	nA_i: 30	xA_i: 2	
Beam $2Theta_i$:	$2Theta_i$ (deg): 0	$T_{i,dist.}$: none	Sigma$T_{i,dist.}$(deg): -	$T_{i,min}$ (deg): -	$T_{i,max}$ (deg): -	nT_i: 10	xT_i: 2	
Substrate:	n-$delta_S$: 3.E-06	n-$beta_S$: 2.8E-8	Layer thickness (nm): 0	n-$delta_L$: 2.E-05	n-$beta_L$: 2.5E-06	RMS roughness(nm): 0.5		
Particle:	n-$delta_I$: 2.E-05	n-$beta_I$: 2.5e-6	Depth(nm): 0	n-$delta_{SH}$: 2.E-05	n-$beta_{SH}$: 2.5E-06			

Particle parameters:

Number of different particle types: 2		Base angle (deg)		Height ratio	Flattening			
Type 1:	Spheroid	54.73		1	*H/R* (spheroid)			
Type 2:	Spheroid	54.73		1	*H/R/2* (hemispheroid)			
Size of particle		Radius (nm)	$R_{dist.}$	SigmaR/R	Rmin(nm)	Rmax(nm)	nR	xR
	Type 1:	*R*	log_normal	$Sigma_R$	0.1	10	25	2
	Type 2:	*R*	log_normal	$Sigma_R$	0.1	10	25	2
Height aspect ratio		Height/R	$H_{dist.}$	SigmaH/H	Hmin(nm)	Hmax(nm)	nH	xH	rhoH
	Type 1:	*1.7*	coupled	-	-	-	25	2	1
	Type 2:	*1.7*	coupled	-	-	-	25	2	1

Lattice parameters:

Particle distribution type: 1DDL						
Interference function:	Peak position D (nm)	w (nm)	Statistics	Eta_Voigt	Size-Distance coupling	Cut-off
	D	*W*	gau	0.5	4	10000000

Table S.1: Input parameters for *IsGISAXS* simulations. The particle radius (R), its distribution ($Sigma_R$), the average center-to-center distance (D) and its distribution (W) were adapted to find the better agreement between acquired and simulated patterns.

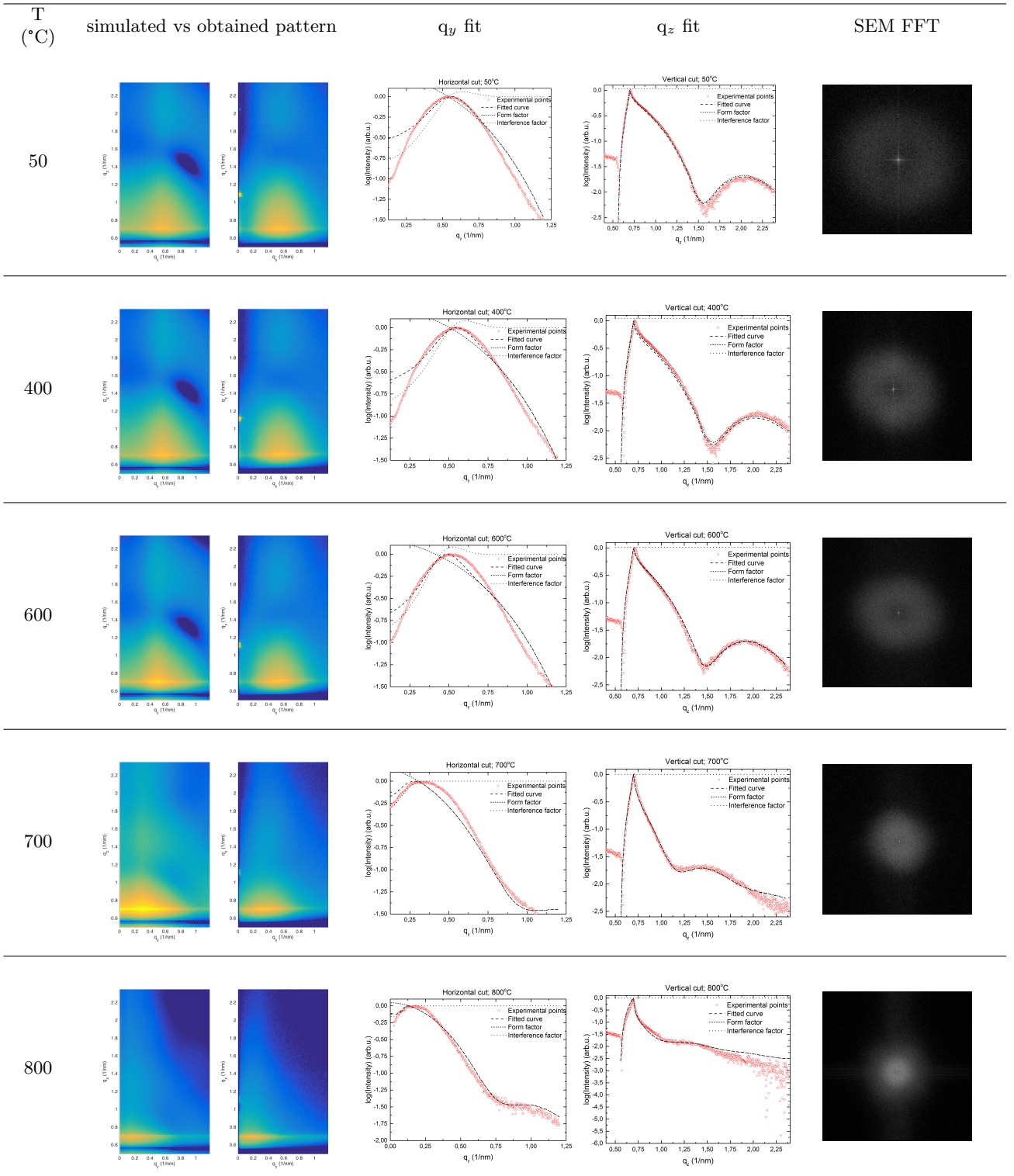

Figure S.2: From left to right: simulated and acquired GISAXS patterns from the as-deposited and a selection of quenched samples during thermal annealing in O_2; fits to the line profiles along q_y and q_z; and FFT images of the corresponding SEM images.

	sample	spacing[1] (nm)			radius (nm)		height (nm)
		analysis	simulated	FFT	analysis	simulated	simulated
SiO_2	as-deposited	11	9.0 ± 1.75	9.7	3.2	3.15	5.35
SiO_2	400 ˚C	11	9.5 ± 1.75	10.0	3.2	3.15	5.35
SiO_2	600 ˚C	11	11.0 ± 2.0	11.0	3.3	3.15	5.35
SiO_2	700 ˚C	18	14.0 ± 4.5	15.3	3.8	3.95	7.11
SiO_2	800 ˚C	35	30.0 ± 12.5	28.2	5.3	4.60	7.82

[1]The calculated spacing was considered as the average particle center-to-center distance between the two closest particle neighbors.

Table S.2: Particle size and spacing data obtained for the as-deposited Pt nanoparticles and quenched samples at selected temperatures via the fast analysis, *IsGISAXS* simulations and FFT analysis of SEM images.

Temperature (˚C)	Particle radius (nm)	σ (nm)
As deposited	3.15	0.53
400	3.15	0.53
600	3.15	0.53
700	3.80	0.69
800	4.6	0.86

Table S.3: Particle size distribution obtained via *IsGISAXS* simulations for the Pt-D sample. A log-normal distribution was determined. The size distribution only increases when particle coarsening occurs.

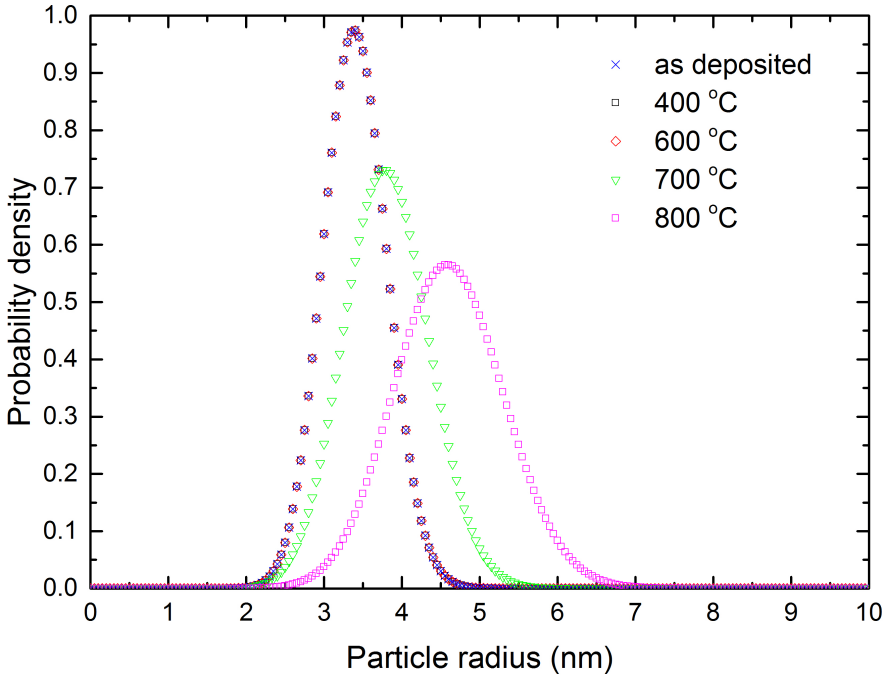

Figure S.3: Log-normal probability distribution curves of the Pt-D particle size obtained via *IsGISAXS* simulations during the annealing process.

3 SEM images and GISAXS patterns

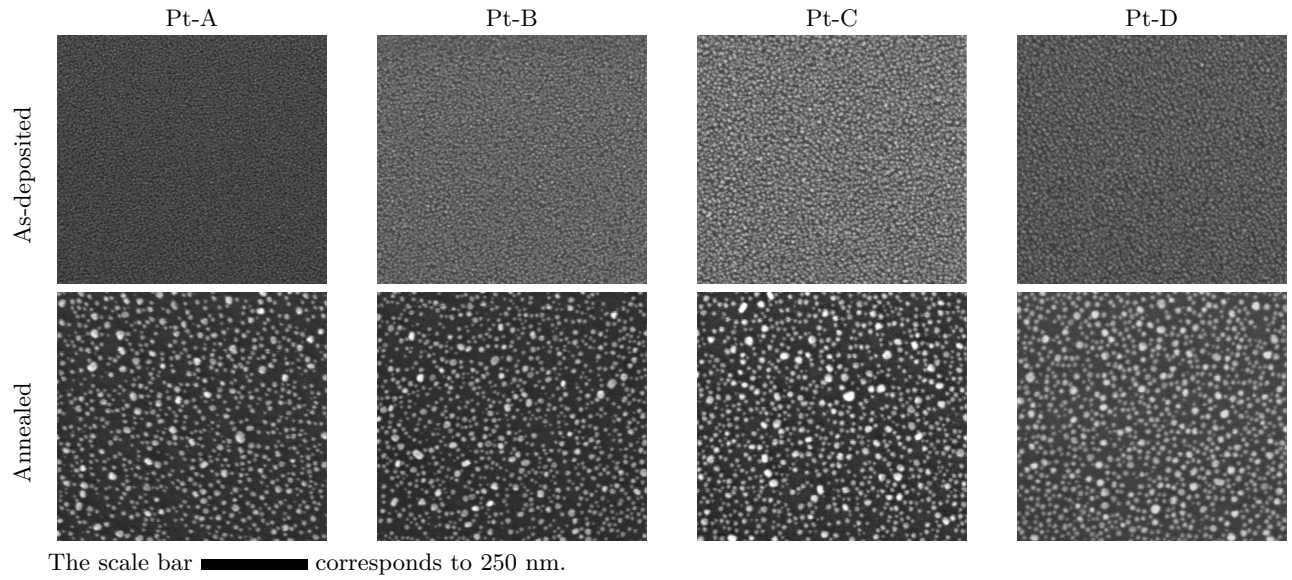

Figure S.4: SEM images of the as-deposited Pt nanoparticles (top) and of the same samples annealed up to 800 °C (0.2 °C/s) under 18 % of O_2 in He (bottom). The initial morphology (particle size and spacing) was demonstrated to be different for the four depositions employing combinations of the O_2 and N_2*-based Pt ALD processes. After the annealing procedure, all four samples exhibit a similar particle morphology.

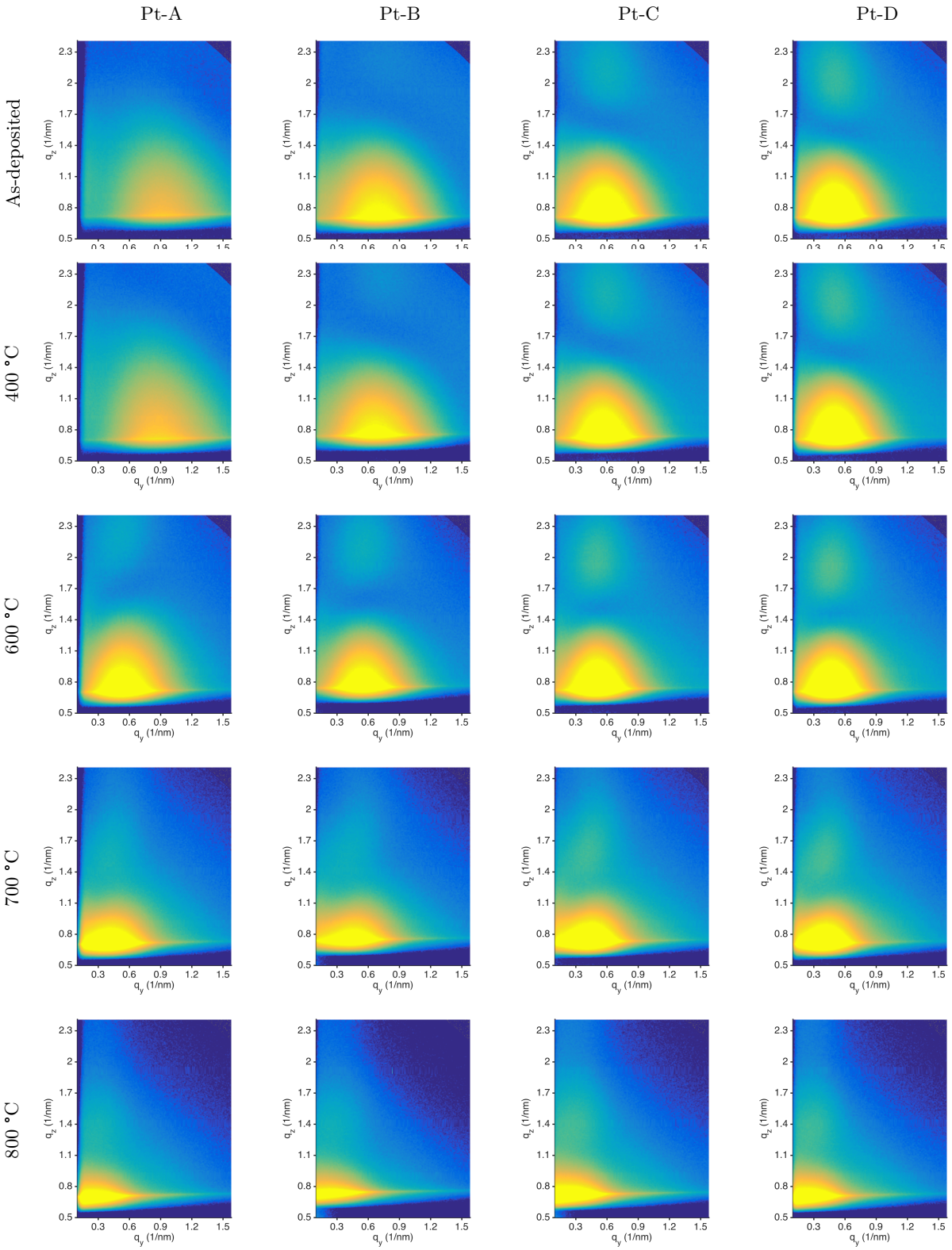

Figure S.5: *In situ* GISAXS images acquired while ramping the temperature at 0.2 °C/s to 800°C in 18 % of O_2 in He. The initial morphology (particle size and spacing) was demonstrated to be different for the four depositions employing combinations of the O_2 and N_2*-based Pt ALD processes. After the annealing procedure, all samples exhibit similar GISAXS patterns, indicating the same particle morphology (in agreement with the SEM pictures in Fig. S.4).

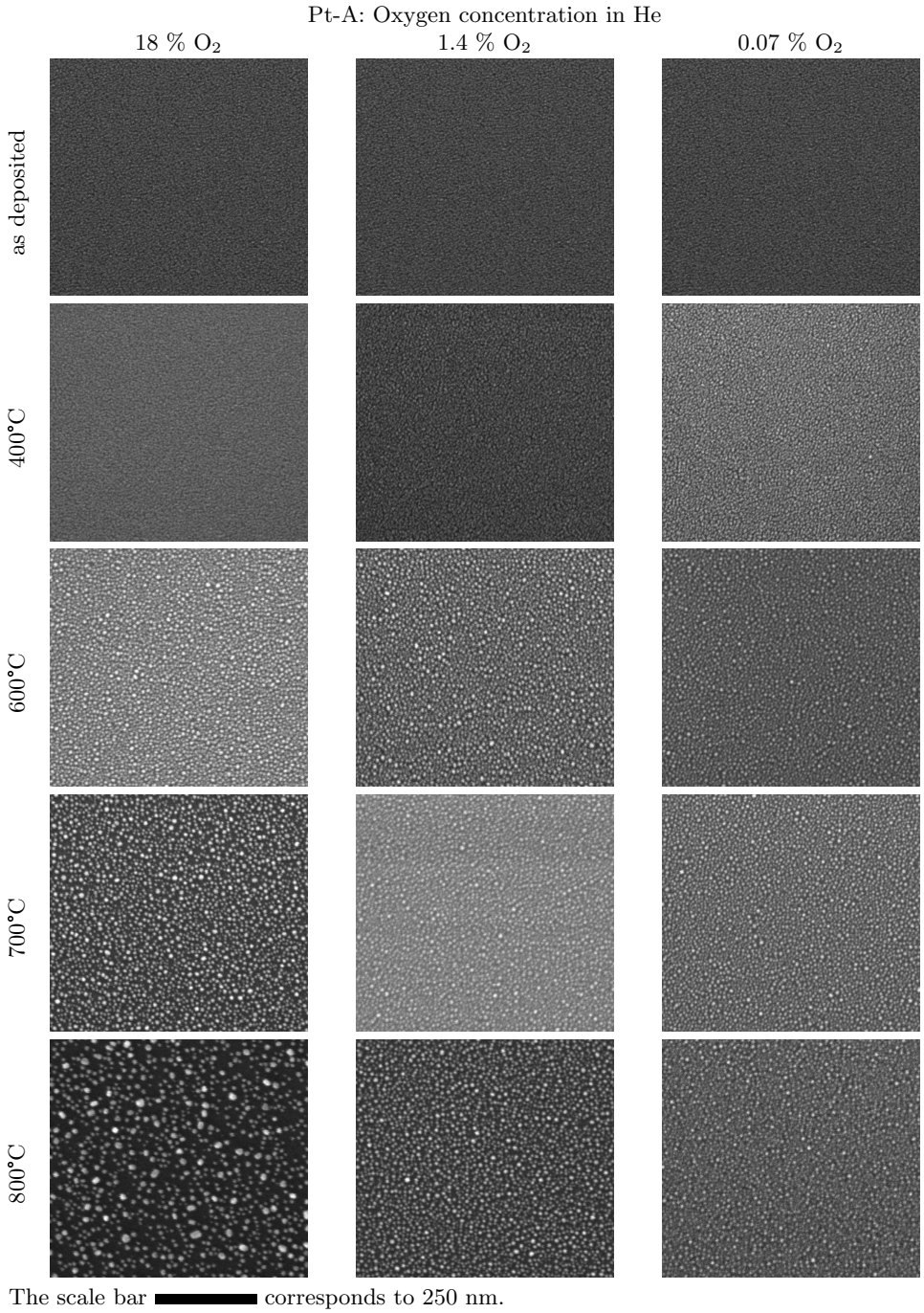

Figure S.6: *Ex situ* SEM images of Pt-A samples quenched at different states during the annealing treatment (0.2 °C/s) under different O_2 partial pressures in He.

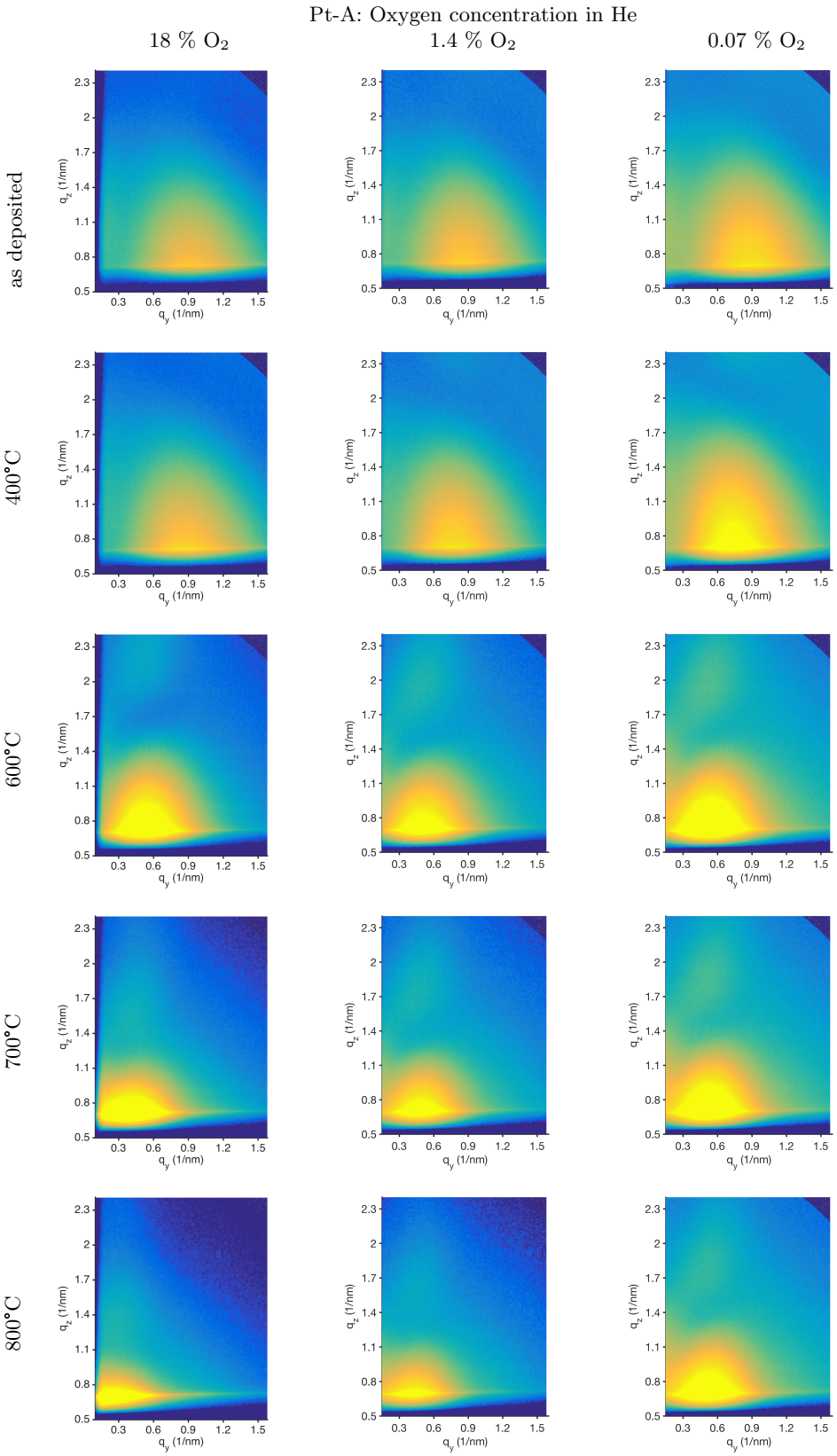

Figure S.7: *In situ* GISAXS images of the Pt-A sample annealed (0.2 °C/s) under different partial pressures of O_2 in He.

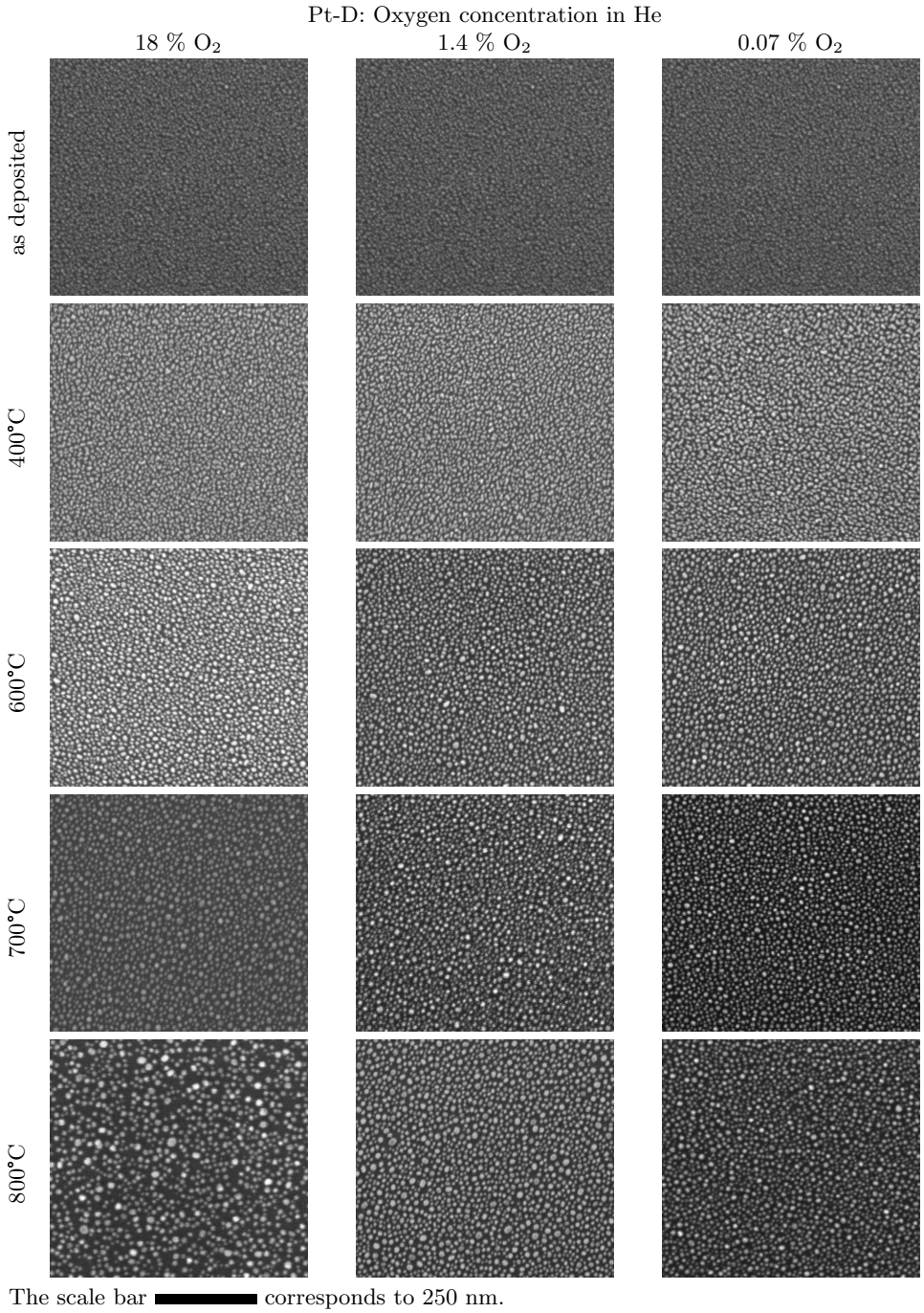

Figure S.8: *Ex situ* SEM images of Pt-D samples quenched at different stages during the annealing treatment (0.2 °C/s) under different O_2 partial pressures in He.

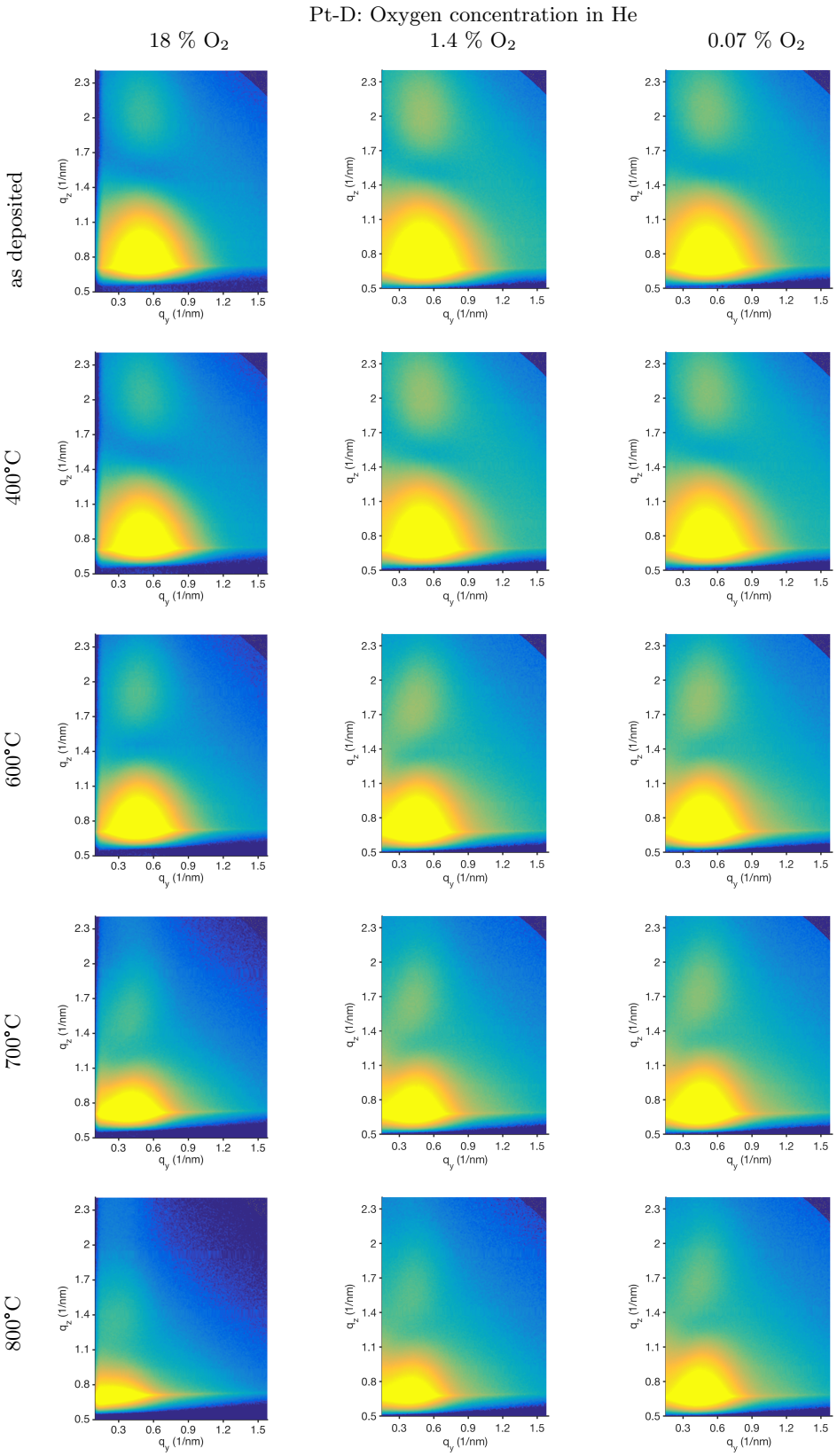

Figure S.9: *In situ* GISAXS images of the Pt-D sample annealed (0.2 °C/s) under different partial pressures of O_2 in He.

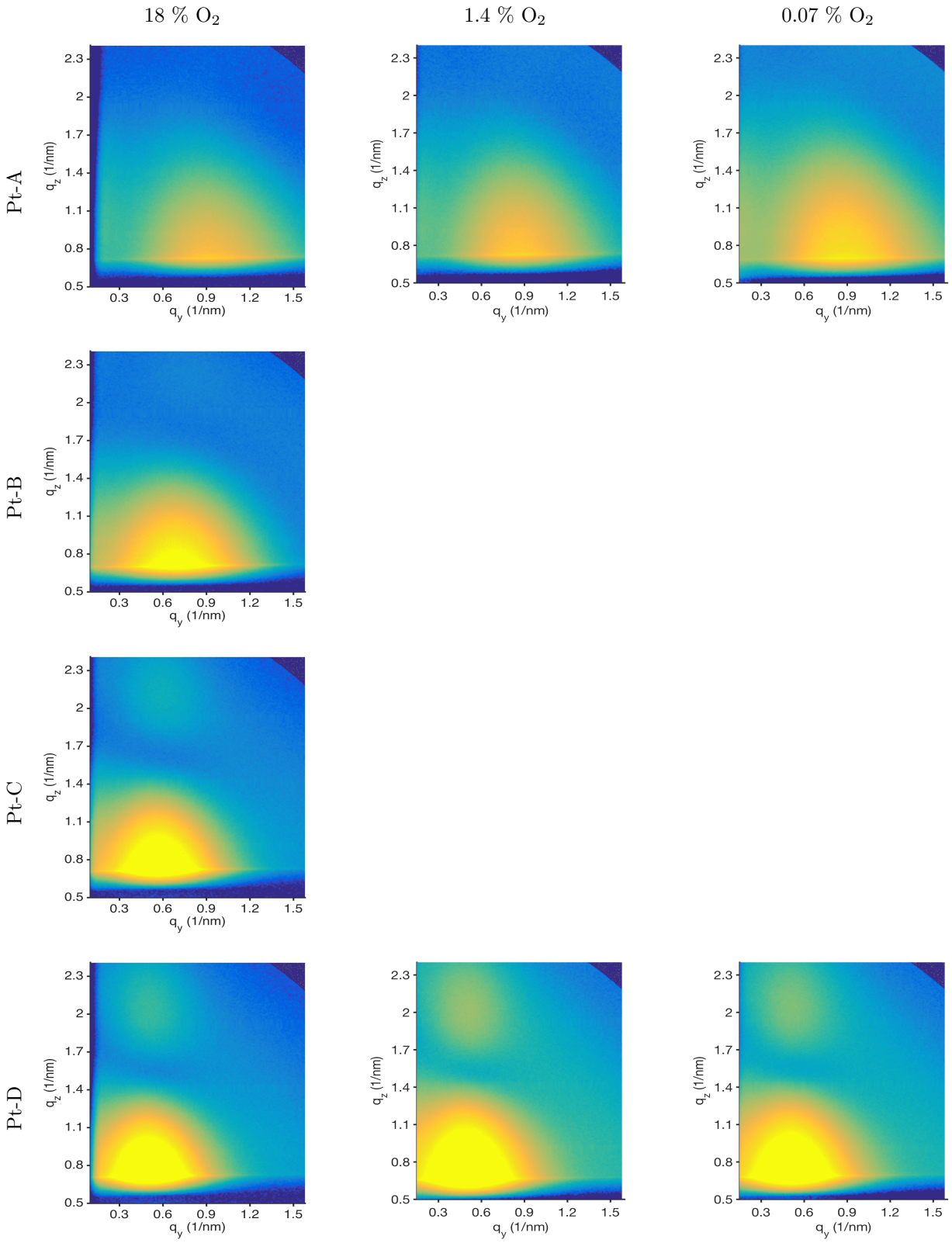

Figure S.10: Digital *.avi* files showing the continuous GISAXS patterns recorded during annealing. (To visualize these files, it is required to open the *.pdf* document with *Adobe Acrobat Reader*. Also available to download).

4 Results for annealing under H_2 reducing atmosphere

A control experiment comprising the annealing of Pt nanoparticles under reducing atmosphere was carried out. The Pt-D sample was similarly annealed under 20 % of H_2 in He atmosphere (1 bar) up to 1000 °C (0.2 °C/s). Fig. S.11 depicts a selection of GISAXS patterns recorded during the experiment. Fig. S.12 compares the particle size evolution during this anneal in reducing atmosphere with the results obtained for annealing under 18 % of O_2 (same data as in Figure 1 c in the main text). Results proved that an oxidizing atmosphere is required for a noticeable particle coarsening, being negligible the particle growth in a reducing atmosphere.

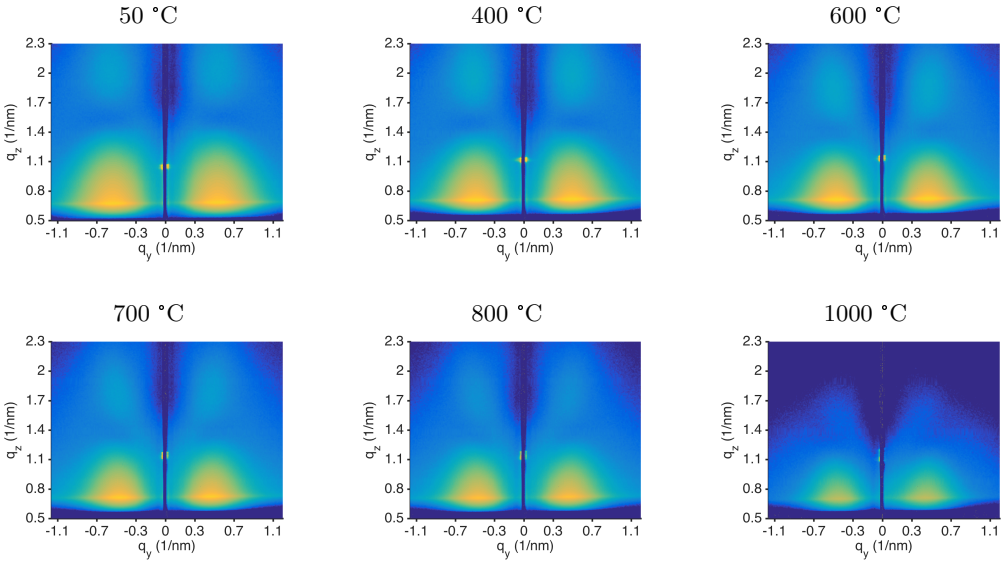

Figure S.11: *In situ* GISAXS images acquired while ramping the temperature at 0.2 °C/s to 1000 °C in 20 % of H_2 in He. No remarkable particle growth was produced. The difference in intensity for higher temperatures is related to very slight changes in the alignment of the sample with respect to the incoming X-ray beam.

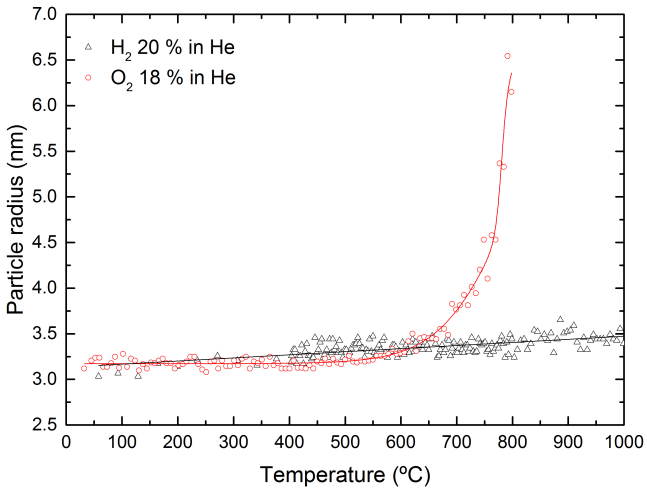

Figure S.12: Comparison of the particle size evolution when annealed in 20 % of H_2 in He (black) and in 18 % of O_2 in He (red). The oxidizing atmosphere has a clear effect on the particle coarsening.

References

[1] R. Lazzari, *J. Appl. Crystallogr.*, 2002, **35**, 406–421.

[2] A. Hexemer and P. Muller-Buschbaum, *IUCrJ*, 2015, **2**, 106–125.